Scavenging the Water Cation in Concentrated Acidic Solutions

ARTICLE *in* THE JOURNAL OF PHYSICAL CHEMISTRY A · OCTOBER 2015

Impact Factor: 2.69 · DOI: 10.1021/acs.jpca.5b07601

3 AUTHORS, INCLUDING:

Jun Ma

Université Paris-Sud 11

15 PUBLICATIONS **79** CITATIONS

SEE PROFILE

Mehran Mostafavi

Université Paris-Sud 11

162 PUBLICATIONS **2,907** CITATIONS

SEE PROFILE

THE JOURNAL OF PHYSICAL CHEMISTRY A

Article

pubs.acs.org/JPCA

Scavenging the Water Cation in Concentrated Acidic Solutions

Jun Ma,[†] Jay A. LaVerne,[‡] and Mehran Mostafavi*[,†]

[†]Laboratoire de Chimie Physique/ELYSE, Univ. Paris-Sud/CNR/Université Paris-Saclay, Orsay 901405, France

[‡]Radiation Laboratory and Department of Physics, University of Notre Dame, Notre Dame, Indiana 46556, United States

ABSTRACT: Picosecond pulse radiolysis techniques were used to observe the kinetics of the $SO_4^{\bullet-}$, $H_2PO_4^{\bullet}$, $Cl_2^{\bullet-}$, and $Br_2^{\bullet-}$ species formed in the fast oxidation of concentrated and highly acidic solutions of SO_4^{2-}, PO_4^{3-}, Cl^-, and Br^-. Experimental results were compared with model predictions to gain insight into the possible mechanisms occurring on the fast time scales. Simple kinetics involving the oxidizing $OH^{\bullet}$ radical formed by radiolytic water decomposition could not account for the observed yields at the very short times (within the electron pulse ~7 ps). Diffusion-kinetic simulations of the spur reactions induced by the incident electrons show that additional oxidation of the solutes must occur at very short times and involves their direct ionization along with scavenging of the highly oxidizing $H_2O^{\bullet+}$ radical formed in the initial ionization of the water medium. The fraction of $H_2O^{\bullet+}$ radicals scavenged varies as 0.26, 0.68, 0.92, and 0.97 for PO_4^{3-}, SO_4^{2-}, Cl^-, and Br^- solutions, respectively. These studies represent the first semiquantitative estimation of the $H_2O^{\bullet+}$ radicals scavenging fractions for such a wide range of solutes.

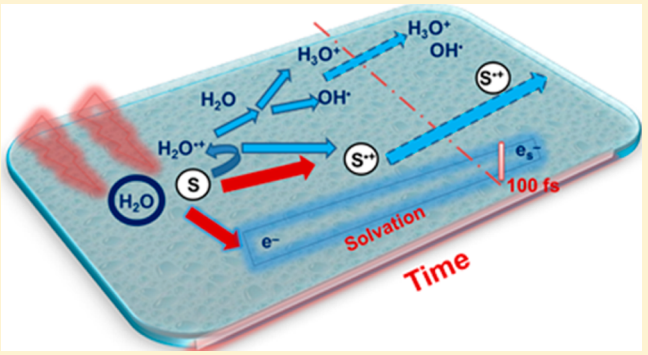

INTRODUCTION

Pulse radiolysis is a well-established technique for the examination of the transient species produced by ionizing radiation, and the chemistry of water and of dilute aqueous solutions has been extensively probed;[1] however, the chemistry occurring in highly concentrated aqueous solutions can be significantly different when compared with water and dilute solutions because scavenging reactions of the solutes can compete with the natural decay of the species produced by water decomposition. Picosecond pulse-probe radiolysis of highly concentrated solutions has shown notable increases in product formation within the electron pulse (7 ps) over that expected from normal oxidation processes.[2−6] The time scales are much too short for reaction kinetics to be responsible for the results, and even direct ionization of the solute cannot solely explain the significant amount of product formation observed within the electron pulse. These results suggest that other oxidation processes must be occurring at very short times in the radiolysis of concentrated aqueous solutions.

Radiation chemistry studies have well established that the deposition of energy by ionizing radiation leads to the formation of the water radical cation, $H_2O^{\bullet+}$, and a free electron.[7] In addition to their recombination, each of these two charged radical species follows its own path of chemical reactivity. On one hand, the electron relaxes toward multiple vibrational modes of water solvent molecules via vibronic coupling and eventually to a localized hydrated electron as the simplest reducing species.[8,9] On the other hand, the $H_2O^{\bullet+}$ radical undergoes proton transfer to give the oxidizing $OH^{\bullet}$ radical. This latter species is responsible for much of the oxidation that occurs in dilute aqueous solutions. Neutralization of $H_2O^{\bullet+}$ radical occurs on the femtosecond time scale so this species is not normally available for reaction;[7,10] however, the probability of an encounter between an $H_2O^{\bullet+}$ radical and a solute molecule is not negligible when the solute concentration is on the same order of magnitude as a water molecule. Not long after the discovery of hydrated electron in 1962, it was assumed by Hamill et al. that holes in water could be trapped prior to hydration using sufficiently high concentrations of solutes such as NaX (X = Cl, Br, F, I) or sulfate salts. The high values for the yields of secondary radicals $Cl_2^{\bullet-}$ or $SO_4^{\bullet-}$ from steady-state scavenger or time-resolved nanosecond pulse radiolysis measurements were attributed partially to electron transfer from $H_2O^{\bullet+}$ radical to anions.[11,12] At low temperature, ESR (electron spin resonance) measurements also showed that electron transfer from the water hole induced in the inner hydration layer of DNA can occur.[13] These early studies proposed that the $H_2O^{\bullet+}$ radical could initiate oxidation processes both in the homogeneous phase and in interfacial biological systems, but the results are very speculative because the time scales for these reactions are very fast (~100 fs). Even picosecond pulse radiolysis studies cannot directly probe the chemistry of the $H_2O^{\bullet+}$ radical; however, the products due to $H_2O^{\bullet+}$ radical oxidation processes can be observed without complications due to longer time chemistry. Previous picosecond pulse radiolysis studies have shown that water cations can involve the fast oxidation reactions of solutes when the ionized water molecule is in contact with ions or molecules.

Received: August 5, 2015
Revised: October 9, 2015
Published: October 9, 2015

DOI: 10.1021/acs.jpca.5b07601
J. Phys. Chem. A 2015, 119, 10629−10636

Table 1. Characteristics of Solutions Including Solute Concentration, Hydronium Ion Concentration, Direct Ionization Yield of the Solute, Electron Fraction of the Water, Water Cation Yield, Molar Ratio of Water to the Solute, and the Fraction of Water Cations Reacting with the Solute

	[S]	$[H_3O^+]$ (M)	G_s ($\times 10^7$ mol/J)	f_w	$G(H_2O^{\bullet+})$ ($\times 10^7$ mol/J)	H_2O/S	α
H_2O	0	10^{-6}		1.0	4.2		
H_2O	0	1.0		1.0	4.2	52.8	
H_2SO_4	10.0	10.1	3.5	0.38	4.8	3.1	0.68
H_3PO_4	11.0	4.18	3.7	0.32	4.8	2.4	0.26
HCl	12.1	12.1	4.35	0.66	4.8	3.4	0.2−1.0
NaCl	5.5	10^{-6}	4.35	0.76	4.8	8.9	0.92
HBr	8.89	8.89	5.0	0.58	4.8	5.3	0.2−1.0
NaBr	6.0	10^{-6}	4.35	0.62	4.8	7.2	0.97

This electron transfer is enhanced with increasing solute concentration.[4−6,14,15] The secondary radicals observed at 15 ps are suggested to be formed by direct ionization and indirect $H_2O^{\bullet+}$ radical oxidation of solutes.

The present study is focused mainly on these fast oxidation pathways through a combination of simulated model predictions and kinetic measurements in a variety of irradiated acidic aqueous solutions. Electrons are produced by direct ionization of the solute and by water radiolysis. Electrons undergo three reactions: recombination with the $H_2O^{\bullet+}$ radical, which is considered to be very fast (less than 1 ps), solvation (also in less than 1 ps), and reaction with H_3O^+ before solvation. The latter process is very important in highly concentrated acidic solutions. Very recently, it was shown that in acidic solutions a pre-$H^\bullet$ atom is formed, which is a very reducing species.[16] The ultrafast processes concerning the dynamics of electrons in neat water and highly acidic solutions have been extensively studied.[17,18] This work is mainly concerned with the short-lived formation of secondary radicals such as $SO_4^{\bullet-}$, $H_2PO_4^\bullet$, $Cl_2^{\bullet-}$, and $Br_2^{\bullet-}$ in concentrated acidic solutions of SO_4^{2-}, PO_4^{3-}, Cl^-, and Br^-, respectively. Model simulations of the radiolysis of neat water and water with 1 M perchloric acid were used to first establish the formation and decay of the $OH^\bullet$ radical and to verify the accuracy of the model. The kinetics of each of the short-lived species in the concentrated acidic solutions was then calculated and compared with experimental observations. Conclusions are then made on the possible mechanisms responsible for the observations.

EXPERIMENTAL SECTION

Pulse Radiolysis. The pulse radiolysis measurements were performed at the ELYSE facility, which is a picosecond electron accelerator based on the radiofrequency photogun technology as fully detailed elsewhere.[19] Electrons were accelerated to 7 MeV energy, and each pulse had a charge of 4 nC at a repetition rate of 10 Hz. Both the electron pump pulses and the optical probe pulses are generated by the same femtosecond laser source, a femtosecond Ti:sapphire laser, to intrinsically synchronize them.

Multiple wavelengths from the UV to the visible were produced simultaneously and used to probe the kinetics of the transients from about 10 to 3800 ps.[20] After passing the optical delay line, two probe beams are generated in a rectangular arrangement before they are unified by a 50% beam splitter. In one arm of the rectangle, a supercontinuum was generated in a CaF_2 disk to probe the absorbance changes from 350 to 800 nm. In the second arm of the rectangle, the second and third harmonic of the initial laser wavelength are generated to probe at 260 nm. Signal beams are coupled in an optic fiber after passing the sample. The signal and the reference beam are transmitted to a spectrometer and dispersed onto a CCD.

Electron pulses and optical probe pulses were collinear through the sample cell. The diameter of the electron bunch at the position of the cell was in the range of 3 to 4 mm, and the sample cell windows were 200 μm thick to reduce their absorption.[14,15] The spatial overlap of the electron beam on the probe beam was optimized using the transient absorption signal of the empty cell. The dose per pulse in pure water was determined by measuring the absorbance of the solvated electron, $A_{e^-_{hyd}}(\lambda, t)$, and by considering its yield measured at 20 ps to be $G(t = 20\ \text{ps}) = 4.25 \times 10^{-7}$ mol/J.[21] Therefore, the dose absorbed in water is given by

$$D_{water}(\text{Gy}) = \frac{A_{e^-_{hyd}}(\lambda, t)}{\varepsilon_\lambda l \rho_w G(t)} \quad (1)$$

where ε is the solvated electron extinction coefficient (19 130 M^{-1} cm^{-1}, at the maximum 718 nm), l is the optical path length, and ρ_w is the density of water. All of the measurements were made in a flow cell with a 5 mm optical path collinear to the electron pulse propagation. The absorbance measured for a given species in highly concentrated solutions is given by eq 2

$$A(\lambda, t) = \varepsilon_\lambda l c(t) = \varepsilon_\lambda l F D_W G(t) \quad (2)$$

where ε_λ is the extinction coefficient at wavelength λ. The dose additionally absorbed by the solute in concentrated solutions (taking HBr solutions as an example) is obtained by multiplying the absorbed dose in pure water by the dose factor F

$$F = \rho_{sol}(Z_{HBr}p/A_{HBr} + Z_{water}(100 - p)/A_{water})(Z_{water}100/A_{water})^{-1} \quad (3)$$

where ρ_{sol} is the density of the solution, Z is the number of electrons, A is the mass number, and p is the weight fraction of the solute per 100 g of solution. Solutions containing solute anions at high concentration and pure water were studied under identical experimental conditions. Particular attention was given to the use of a constant dose per pulse. Measurements were performed at 22.5 °C, the room temperature during the pulse radiolysis experiments. The transient signals due to the cell are considered for kinetics recorded in solutions to avoid important errors on the time-dependent yield of transient species, particularly of those absorbing in the UV.

Chemical reagents were the highest quality available from Sigma-Aldrich and used as received. Water was purified by passage through a Millipore purification system. The solutions

DOI: 10.1021/acs.jpca.5b07601
J. Phys. Chem. A 2015, 119, 10629−10636

Table 2. Reaction Schemes Used for the Oxidation of PO_4^{2-} and SO_4^{2-}

	reaction	k (M^{-1} s^{-1})
S1	H_2SO_4, HSO_4^-, $SO_4^{2-} \rightarrow H_2SO_4^{\bullet+}$, $HSO_4^{\bullet}$, $SO_4^{-\bullet} + e^-$	
S2	H_2SO_4, HSO_4^-, $SO_4^{2-} + H_2O^{\bullet+} \rightarrow H_2SO_4^{\bullet+}$, $HSO_4^{\bullet}$, $SO_4^{-\bullet} + H_2O$	
S3	$OH^{\bullet} + H_2SO_4 \rightarrow HSO_4^{\bullet} + H_2O$	1.4×10^7
S4	$OH^{\bullet} + HSO_4^- \rightarrow SO_4^{\bullet-} + H_2O$	4.7×10^5
S5	$SO_4^{\bullet-} + H^{\bullet} \rightarrow HSO_4^-$	1.0×10^{10}
S6	$SO_4^{\bullet-} + SO_4^{\bullet-} \rightarrow S_2O_8^-$	7.6×10^8
S7	$SO_4^{\bullet-} + OH^{\bullet} \rightarrow HSO_5^-$	1.0×10^9
S8	$SO_4^{\bullet-} + S_2O_8^{2-} \rightarrow S_2O_8^- + SO_4^{2-}$	6.6×10^5
S9	$SO_4^{\bullet-} + HO_2^{\bullet} \rightarrow O_2 + HSO_4^-$	3.5×10^9
S10	$H^{\bullet} + S_2O_8^{2-} \rightarrow SO_4^{\bullet-} + HSO_4^-$	2.5×10^7
S11	$H^{\bullet} + HSO_5^- \rightarrow SO_4^{\bullet-} + H_2O$	2.2×10^8
P1	H_3PO_4, $H_2PO_4^-$, HPO_4^{2-}, $PO_4^{3-} \rightarrow H_3PO_4^{+\bullet}$, $H_2PO_4^{\bullet}$, $HPO_4^{\bullet-}$, $PO_4^{\bullet2-} + e^-$	
P2	H_3PO_4, $H_2PO_4^-$, HPO_4^{2-}, $PO_4^{3-} + H_2O^{\bullet+} \rightarrow H_3PO_4^{+\bullet}$, $H_2PO_4^{\bullet}$, $HPO_4^{\bullet-}$, $PO_4^{\bullet2-} + H_2O$	
P3	$OH^{\bullet} + H_3PO_4 \rightarrow H_2PO_4^{\bullet} + H_2O$	4.2×10^4
P4	$OH^{\bullet} + H_2PO_4^- \rightarrow HPO_4^{\bullet-} + H_2O$	2.0×10^4
P5	$H_2PO_4^{\bullet-} + H^{\bullet} \rightarrow H_3PO_4$	1.3×10^{10}
P6	$H_2PO_4^{\bullet-} + H_2PO_4^{\bullet-} \rightarrow H_4P_2O_8$	2.5×10^9
P7	$H_2PO_4^{\bullet-} + OH^{\bullet} \rightarrow H_3PO_5$	4.0×10^9
P8	$H_2PO_4^{\bullet-} + HO_2^{\bullet} \rightarrow H_3PO_4 + O_2$	3.0×10^9
P9	$H_2PO_4^{\bullet-} + H_2O_2 \rightarrow H_3PO_4 + HO_2^{\bullet}$	3.5×10^9

were air saturated and they were prepared at different concentrations and pH, as listed in Table 1. Solutions containing anions at high concentration and neat water were studied under identical experimental conditions. The temporal evolution of each sample under investigation was scanned on the order of 10 times with a single point averaging of 5 to 20 time intervals for each delay step.

Diffusion-Kinetic Methodology. Kinetic modeling of the chemistry induced by fast electrons cannot be performed in concentrated solutions without explicit cross sections for the energy-loss processes and fragmentation mechanism for each solute, which are generally unknown. Therefore, the chemistry of an isolated spur representative of fast electrons was examined in exactly the same manner as previously done with concentrated Br^- and Cl^- solutions.[5,6] This method employs a nonhomogeneous deterministic model in which the coupled differential equations for the various reactions were stepped in time using FACSIMILE, which is based on the Gear algorithm.[22] Water reactions, rate coefficients, and diffusion coefficients for the water generated species are the same as previously used.[23] The initial Gaussian spatial distributions were normalized using neat water radiolysis to give reasonable agreement with the reported yields of 4.80×10^{-7} mol/J for the $OH^{\bullet}$ radical at 10 ps[24] and 4.25×10^{-7} mol/J for the hydrated electron at 20 ps[21] and by matching the observed decay of these two species in pure water up to 1 μs. Goodness of fit of the pure water reactions to the available data can be observed in the previous work.[5] Reactions included with the water chemistry in the oxidation of Br^- and Cl^- solutions were as previously reported.[5,6] Rate constants for the $Cl_2 + Cl^- \rightarrow Cl_3^-$, $Cl_3^- \rightarrow Cl_2 + Cl^-$, $Br_2 + Br^- \rightarrow Br_3^-$, and $Br_3^- \rightarrow Br_2 + Br^-$ reactions were changed to 2×10^4, 1.1×10^5, 1.6×10^8, and 1.0×10^7 M^{-1} s^{-1}, as suggested in a newer reference.[25] The equilibrium constants for these reactions are the same as previously used, and no difference is observed in the kinetics on the time scales considered here. In addition to the water product reactions, the reactions in Table 2 were included for either the PO_4^{3-} or SO_4^{2-} systems. Rate constants used for these additional reactions were as found in the literature.[26,27] The diffusion coefficients used were 2.1, 1.0, 1.2, 1.1, and 1.1×10^{-5} cm^2/s for $Br^{\bullet}$, $Br_2^{\bullet-}$, Br_3^-, $BrOH^{\bullet-}$, and Br_2, respectively; 2.1, 1.2, 1.2, 1.1, and 1.1×10^{-5} cm^2/s for $Cl^{\bullet}$, $Cl_2^{\bullet-}$, Cl_3^-, $ClOH^{\bullet-}$, and Cl_2, respectively; 2.1×10^{-5} cm^2/s for $H_2PO_4^{\bullet}$; and 1.2, 1.1, and 1.1×10^{-5} cm^2/s for SO_4^-, $S_2O_8^{2-}$, and HSO_5^-, respectively.

No attempt was made to model subpicosecond kinetics because of inherent limitations in the approach, so these yields were included in the model before reactions were allowed to commence. Observed yields, G_{obs}, were determined from

$$G_{obs} = f_s G_s + f_w G_{H_2O^{\bullet+}} \alpha \quad (4)$$

where f_s is the electron fraction of the solute, G_s is direct ionization yield of the solute, f_w (= 1 − f_s) is the electron fraction of the water, $G_{H_2O^{\bullet+}}$ is the yield of water cations formed, and α is the fraction of water cations that react with the solute. Electron fractions were obtained from the molarities of the solutions, and the values are given in Table 1. The radiation chemical yield for the direct ionization for Cl^- and Br^- was assumed to be the same as for the ionization of water except for highly concentrated acidic Br^- solutions, and further discussion is given below. Direct ionization yields for SO_4^{2-} and PO_4^{3-} were taken to be 3.5 and 3.7 mol/J, respectively, as determined from direct measurements of neat H_2SO_4 and H_3PO_4 acids.[14,15] The values of $G_{H_2O^{\bullet+}}$ and α cannot be determined independently, so they were chosen to best fit the experimental data with some physical limitations on both. Scavenging of the $H_2O^{\bullet+}$ radical was offset by an equivalent adjustment of the $OH^{\bullet}$ radical yield.

RESULTS AND DISCUSSION

Water Radiolysis. The work presented here focuses on the oxidation of solutes by water radiolysis products, especially those processes that occur on very short times (within the electron pulse ~7 ps). Most of the oxidation in dilute solutions is due to the $OH^{\bullet}$ radicals produced on the nanosecond or microsecond time scale. The normal formation of the oxidizing

DOI: 10.1021/acs.jpca.5b07601
J. Phys. Chem. A 2015, 119, 10629−10636

species and their subsequent reactions in water and in dilute aqueous solutions are

$$H_2O \rightarrow H_2O^{\bullet+} + e^- \quad (5)$$

$$H_2O^{\bullet+} + H_2O \rightarrow OH^{\bullet} + H_3O^+ \quad (6)$$

$$OH^{\bullet} + S \rightarrow SOH^{\bullet} \rightarrow S^{\bullet+} + OH^- \quad (7)$$

where the solute S is transformed to its oxidized form $S^{\bullet+}$, which can go on to initiate further chemistry. Under the normal conditions in dilute aqueous solutions, reaction 7 would occur on the time scales of a few nanoseconds to milliseconds depending on the concentration of S and the rate constant for this reaction.

Solute molecules can be oxidized by two methods that do not involve chemistry due to the $OH^{\bullet}$ radical: direct ionization and by reaction with the $H_2O^{\bullet+}$ radical. Charged particles such as fast electrons lose energy through Coulombic interactions with electrons of the medium molecules. Energy deposition by ionizing radiation to a system consisting of several constituents will be initially distributed according to the electron fraction of each component. At solute concentrations of a few molar or more a substantial fraction of the initial energy deposition will directly ionize the solute molecules instead of the water

$$S \rightarrow S^{\bullet+} + e^- \quad (8)$$

to give the oxidized solute and a free electron. The $H_2O^{\bullet+}$ radical is a highly oxidizing species, and the proton transfer by reaction 6 usually occurs within 100 fs in neat water; however, oxidation of the solute by $H_2O^{\bullet+}$ radical can occur at high solute concentrations.

$$H_2O^{\bullet+} + S + H_2O \rightarrow S^{\bullet+} + H_3O^+ + OH^- \quad (9)$$

The net outcome of reactions 8 and 9 are identical to the sequence of reactions 5−7; however, both reactions 8 and 9 are fast processes, and the products of the solute oxidation will be available for subsequent reactions on a much shorter time scale than normally occurring. Note that there might also be other possible fast oxidation processes occurring. The electronically excited states, H_2O^*, are known to dissociate, as in vapor phase, mainly into oxidizing $OH^{\bullet}$ and $H^{\bullet}$ radicals that might further induce oxidation of solutes in acidic solutions, but the contribution of this channel is much less important than the ionization of the water molecule. Besides, if the electron is ejected from the core-level orbitals of the water molecule by high-energy radiation; then, the Auger process is likely to take place, resulting in the formation of higher charged species, denoted as H_2O^{2+}; however, the cross section for this ionizing process is considered to be very low in the case of fast electron radiolysis. Therefore, picosecond electron pulse radiolysis techniques combined with model predictions can be used to estimate the overall solute oxidation at short times.

Diffusion-kinetic simulations of the spur reactions induced by the incident electrons were performed to match the kinetics observed initially following the pulse. Stochastic kinetic models are very meticulous and require energy loss cross sections and fragmentation patterns of the major components in the medium. Direct solute radiolysis processes in dilute aqueous solutions can be ignored, but such is not the case when the solute concentrations are on the same order of magnitude as the water. Because most of the necessary cross sections for solutes are not available, a deterministic approach has been used. This methodology essentially uses an average spur rather than averaging the results of many stoichiometric simulations. The results for $OH^{\bullet}$ radical kinetics are shown in Figure 1 for

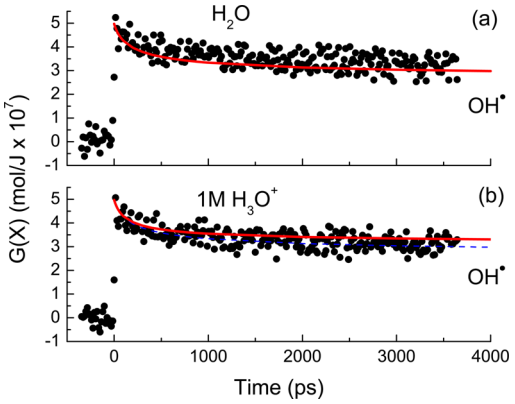

Figure 1. Radiation chemical yields of $OH^{\bullet}$ radical in (a) neat water (●) with model prediction (solid line) and in (b) 1 M H_3O^+ solutions of perchloric acid (●) with model predictions for acid (solid line) and neat water (dashed line).

neat water and 1 M perchloric acid solutions. The model faithfully reproduces the short time kinetics as well as the long time escape yield of the $OH^{\bullet}$ radical. Direct measurements give a yield of 4.80×10^{-7} mol/J for the $OH^{\bullet}$ radical at 10 ps and the model predicts a value of 4.85×10^{-7} mol/J.[24] Note that there is considerable fast decay on the first few picoseconds and the model predicts a yield of 5.0×10^{-7} mol/J for the $OH^{\bullet}$ radical at 1 ps. The kinetics for the $OH^{\bullet}$ radical in neat water is also shown with the results for the acid solution for comparison. The formation of the $OH^{\bullet}$ radical is the same in both systems, but the decay of the $OH^{\bullet}$ radical is clearly slower in acid solutions. In neat water, the main reaction of the $OH^{\bullet}$ radical is with the hydrated electron. Conversion of the hydrated electron to $H^{\bullet}$ atoms in acid solution leads to a slower decay of the $OH^{\bullet}$ radical because of the corresponding slower rate coefficient.

Transient Spectra. Picosecond pulse radiolysis techniques were used to probe the formation of the short-lived species $OH^{\bullet}$, $SO_4^{\bullet-}$, $H_2PO_4^{\bullet}$, $Cl_2^{\bullet-}$, and $Br_2^{\bullet-}$ in the radiolysis of water and concentrated solutions of SO_4^{2-}, PO_4^{3-}, Cl^-, and Br^-, respectively. The absorption spectra in different acidic solutions were obtained at the delay time of 15 ps following the electron pulse and shown with that for the $OH^{\bullet}$ radical in Figure 2. All transient radicals spectra are in agreement with previous studies by photolysis and radiolysis. Radicals $SO_4^{\bullet-}$ and $H_2PO_4^{\bullet}$ have broad absorptions with maxima at 450 and 520 nm, respectively. Radicals $Br_2^{\bullet-}$ and $Cl_2^{\bullet-}$ exhibit a sharp absorption located at 360−380 nm, leaving a long tail in the visible range. As the $OH^{\bullet}$ radical absorbs in the deep UV that is beyond our optical detection, its spectrum is taken from the literature.[28,29] In this work, a probe light at 260 nm was selected for recording the kinetics of $OH^{\bullet}$ radical. The hydrated electron is totally scavenged by the acid (H_3O^+) when the concentration of H_3O^+ is above 6 mol L^{-1} as previously described, and its contribution to the observed spectra is small and subtracted out using simultaneous measurements at 600 nm.

Solutions of SO_4^{2-} and PO_4^{3-}. Solutions of 10 M SO_4^{2-} containing 10.1 M H_3O^+ and 11 M PO_4^{3-} with 4.18 M H_3O^+ were irradiated and the temporal dependence of the spectra maxima of $SO_4^{\bullet-}$ and $H_2PO_4^{\bullet}$, respectively, were collected and given in Figure 3. Also, given in this figure are the results of the

DOI: 10.1021/acs.jpca.5b07601
J. Phys. Chem. A 2015, 119, 10629−10636

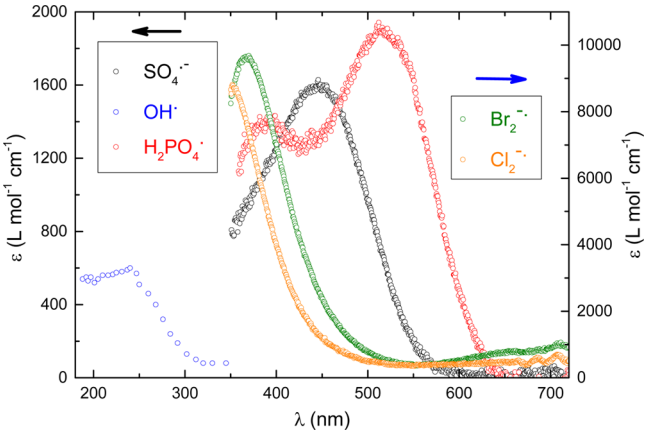

Figure 2. Transition absorption spectrum of the oxidizing species $SO_4^{\bullet-}$, $H_2PO_4^{\bullet}$, $Br_2^{\bullet-}$, and $Cl_2^{\bullet-}$ observed in the various highly concentrated acid solutions by the pulse probe method at 15 ps after the electron pulse with the previously published spectrum of the $OH^{\bullet}$ radical.[28,29]

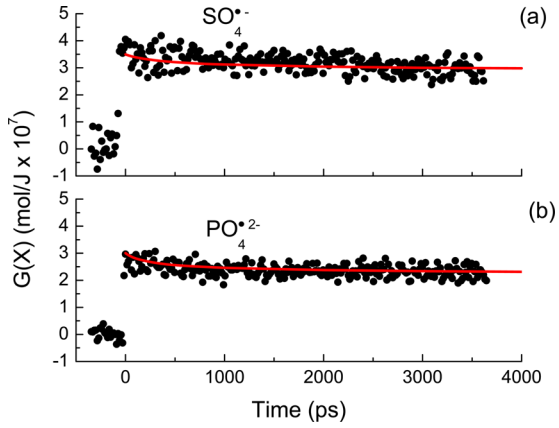

Figure 3. Temporal dependences of the observed radiation chemical yields of (a) $SO_4^{\bullet-}$ (●) and (b) $H_2PO_4^{\bullet}$ (●) with the model predictions (solid lines) using the parameters in Table 1.

model calculations, which are shown to match well with the data. The decay of the oxidized species at short times is due to the bimolecular reactions of $SO_4^{\bullet-}$ + $SO_4^{\bullet-}$ and $H_2PO_4^{\bullet}$ + $H_2PO_4^{\bullet}$, respectively. Both of these systems are somewhat simple at short times in that there is negligible contribution to formation of the oxidized species from reactions with $OH^{\bullet}$ radical on the picosecond time scale. Reactions of the $OH^{\bullet}$ radical in reactions S3, S4, P3, and P4 will occur on the tens of microseconds time scale under the conditions examined here. The formation of the species observed in Figure 3 for the oxidized products $SO_4^{\bullet-}$ and $H_2PO_4^{\bullet}$ on the picosecond time scale must be through direct processes.

Yields of the $SO_4^{\bullet-}$ and $H_2PO_4^{\bullet}$ due to direct ionization of the solutes in concentrated SO_4^{2-} and PO_4^{3-} solutions have been directly measured to be 3.5 and 3.7 × 10^{-7} mol/J in neat acids, respectively.[14,15] The contribution to the observed yield by direct ionization for these two systems is then determined by the first part of eq 4 (f_s G_s) to be 2.2 and 2.5 × 10^{-7} mol/J, respectively. The data show that the picosecond yields are about 3.5 × 10^{-7} mol/J for $SO_4^{\bullet-}$ and 3.0 × 10^{-7} mol/J for $H_2PO_4^{\bullet}$. Obviously, another oxidization process must be occurring. The contribution of the $H_2O^{\bullet+}$ radical was determined by varying the second term of eq 4 (f_w $G_{H_2O^+}$ α) in the kinetic model to match the experimental results. The values of $G_{H_2O^{\bullet+}}$ and α cannot be determined separately with the available information so $G_{H_2O^{\bullet+}}$ was fixed at 4.8 × 10^{-7} mol/J. No one really knows the initial yield of the $H_2O^{\bullet+}$ radical because geminate recombination will instantly convert some of it back to water. The model fit to the data of Figure 1 requires a 1 ps $OH^{\bullet}$ radical yield of 5.0 × 10^{-7} mol/J. This yield can be somewhat higher at even shorter times when solute scavenging occurs. A value of 4.8 × 10^{-7} mol/J for the yield of the $H_2O^{\bullet+}$ radical is not unreasonable, even though it is higher than the 1 ps yield of the hydrated electron, as discussed later. One must realize that scavenging by the solute will occur before 1 ps when the yield of the $H_2O^{\bullet+}$ radical can be considerably higher than the observed hydrated electron yield at 1 ps. Comparison of the model results with the experimental data is best when values of α are taken to be 0.26 and 0.68 for $SO_4^{\bullet-}$ and $H_2PO_4^{\bullet}$, respectively, as given in Table 1 and shown in Figure 3. The error limits for the values of α are different depending on the sensitivity of the system but estimated to be ∼5% for the specific values given here. The relative amount of $H_2O^{\bullet+}$ radical scavenging between these two systems agrees with previous observations,[14,15] but a more quantitative value can now be assessed to the $H_2O^{\bullet+}$ radical contribution to the solute oxidation. This contribution is not negligible because a significant fraction of $H_2O^{\bullet+}$ radicals is oxidizing the solute with a concurrent loss in $OH^{\bullet}$ radical yields.

Solutions of Cl^- and Br^-. Concentrated halide solutions were irradiated at 12.1 M Cl^- and 8.89 M Br^- and the temporal dependences of the $Cl_2^{\bullet-}$ and $Br_2^{\bullet-}$ species, respectively, were recorded at the absorption maxima. In highly acidic solutions, the $XOH^{\bullet-}$ radicals react with the hydronium cation (H_3O^+) very fast (>10^{10} M^{-1} s^{-1}) to form the bromine and chlorine atoms ($X^{\bullet}$) that react with another X^- to produce $X_2^{\bullet-}$. The resulting decay kinetics are shown in Figures 4 and 5 along with the model predictions. The agreement between the model predictions and observed results is reasonable and the fast decay seen at short times is due to the bimolecular $Cl_2^{\bullet-}$ + $Cl_2^{\bullet-}$ and $Br_2^{\bullet-}$ + $Br_2^{\bullet-}$ reactions. There is no measured value for the direct ionizations yield, G_s, for these two solutes, so a value of 4.35 × 10^{-7} mol/J was assumed based on the initial

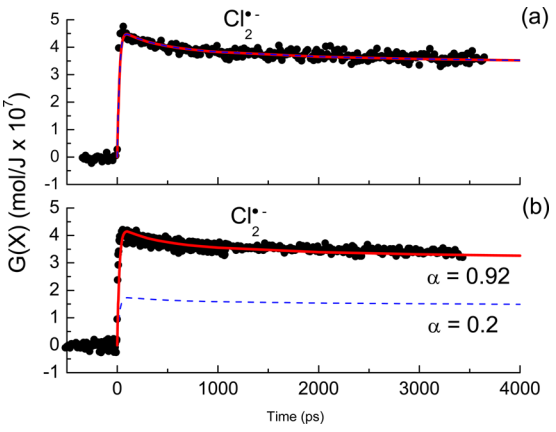

Figure 4. Temporal dependences of the observed radiation chemical yields of $Cl_2^{\bullet-}$ (●) (a) in HCl solutions at 12.1 M Cl^- and 12.1 M H_3O^+ and (b) in NaCl solutions at 5.5 M Cl^- and 1 × 10^{-6} M H_3O^+. Model predictions are given in (a) for α = 1.0 (solid line) and for α = 0.2 (dashed line) and in (b) for α = 0.92 (solid line) and for α = 0.2 (dashed line). Other parameters are as listed in Table 1.

DOI: 10.1021/acs.jpca.5b07601
J. Phys. Chem. A 2015, 119, 10629−10636

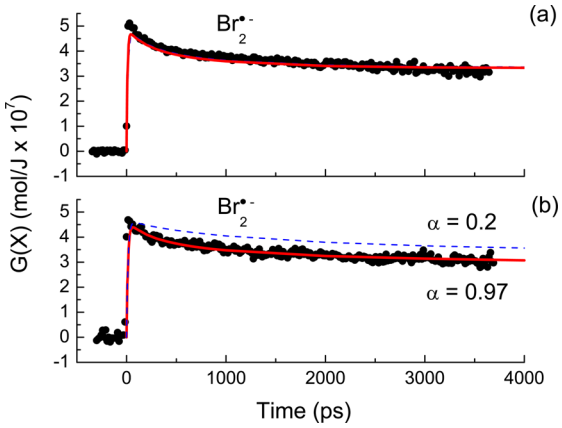

Figure 5. Temporal dependences of the observed radiation chemical yields of $Br_2^{\bullet-}$ (●) (a) in HBr solutions at 8.89 M Br^- and 8.89 M H_3O^+ and (b) in NaBr solutions at 6.0 M Br^- and 1×10^{-6} M H_3O^+. Model predictions are given in (a) for $\alpha = 1.0$ (solid line) and for $\alpha = 0.2$ (dashed line) and in (b) for $\alpha = 0.97$ (solid line) and for $\alpha = 0.2$ (dashed line). Other parameters are as listed in Table 1.

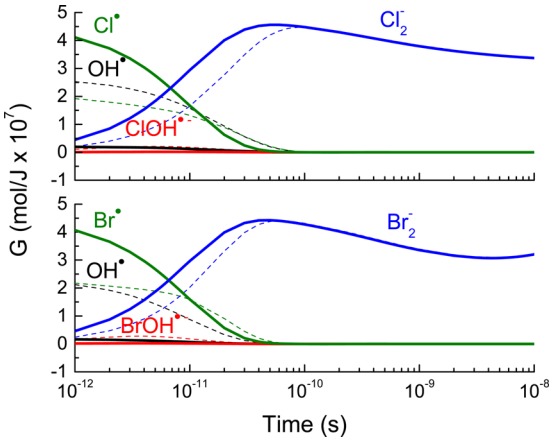

Figure 6. Model predictions for the temporal dependences of the radiation chemical yields of (a) $OH^•$, $Cl^•$, $ClOH^{•-}$, and Cl_2^- in acidic Cl^- solutions and (b) $OH^•$, $Br^•$, $BrOH^{•-}$, and Br_2^- in acidic Br^- solutions. Solid lines are for $\alpha = 1.0$ and dashed lines are for $\alpha = 0.2$. Other parameters are as listed in Table 1.

parameters used in the model calculations. This value for the direct ionization of the halides is the same as that for water giving the hydrated electron. The model predicts a yield for the hydrated electron of 4.3×10^{-7} mol/J at 10 ps, which is in good agreement with the measured value of 4.25×10^{-7} mol/J at this time.[21] Using a similar value for the direct ionization yield of Br^- gave significantly lower predicted yields at short times than observed experimentally, so the direct ionization yield of Br^- was assumed to be 5.0×10^{-7} mol/J. The results of the model predictions are given in Figures 4 and 5 with the observed data. The agreement of the model with the observed $Cl_2^{•-}$ data is very good, while the predicted yield of $Br_2^{•-}$ is still a little low but reasonable. A much higher value for the direct ionization of Br^- becomes more difficult to rationalize, and the reason for the small discrepancy is not known.

Direct ionization processes leading to the formation of $Cl_2^{•-}$ and $Br_2^{•-}$ have yields of 2.8 and 3.1×10^{-7} mol/J, respectively. These yields are again far lower than the observed yields of 4.3 and 4.5×10^{-7} mol/J. Oxidation by the $H_2O^{•+}$ radical is suspected to be responsible for the rest of the observed yields. As suggested from the results on the observations of the $SO_4^{•-}$ and $H_2PO_4^•$ species, a value of 4.8×10^{-7} mol/J was assumed for the yield of the $H_2O^{•+}$ radical; however, the value of α in both systems could be varied from 0.2 to 1.0 with little observable effect on the predicted yields, as shown in Figures 4 and 5. Further evaluation of the kinetics using the model found that oxidation by the $H_2O^{•+}$ radical and the $OH^•$ radical were occurring on essentially the same time scales in acid solutions. The model predictions for the temporal variations of the $OH^•$, $X^•$, $XOH^{•-}$, and X_2^-, where X = Cl or Br, are shown in Figure 6. The $OH^•$ radical initially adds to the halide anion, X^-, to give $XOH^{•-}$, which is in equilibrium with several decay products; however, at the high acid and solute concentrations used here the $XOH^{•-}$ species rapidly undergoes an abstraction by H_3O^+ to the give the $X^•$ radical that immediately reacts with X^- to give $X_2^{•-}$. There is only a very short time window where one can possibly determine the relative contribution of the $H_2O^{•+}$ radical. Therefore, one cannot use these very acidic halide solutions for determination of the contribution of the $H_2O^{•+}$ radical to the fast oxidation of the solutes

Previous picosecond studies examined the oxidation of concentrated solutions of Cl^- and Br^- on fast time scales in near-neutral solutions, and the results are shown in Figures 4 and 5, respectively.[4,5] Results from the model agree well with the experimental data for both sets of data using the parameters in Table 1. Without the high acid concentration, one would expect the $XOH^{•-}$ species to produce the halide radical on a much longer time scale than found in acid solutions. As observed with the analysis of the $SO_4^{•-}$ and $H_2PO_4^•$ species in concentrated highly acidic solutions, variation of the values of α gave different results for the predicted formation of the oxidized species. The contribution of the $H_2O^{•+}$ radical to the fast oxidation of the halides was best matched to the observations using α values of 0.92 and 0.97 for $Cl_2^{•-}$ and $Br_2^{•-}$, respectively. The results are shown in Figures 4 and 5, where it is noticed that lower values of α lead to higher predicted yields. This result is due to the time scales of the formation of $Cl_2^{•-}$ and $Br_2^{•-}$. When these species are formed on extremely fast time scales they are in close proximity to each other and the relatively high concentrations drive bimolecular combination processes. The formation of these species through the $OH^•$ radical allows time for diffusion out of the spur, resulting in lower concentrations of the oxidized species. The values of α for both the Cl^- and Br^- are extremely large and suggest that a large fraction of the H_2O^+ radicals are scavenged in these systems.

■ CONCLUSIONS

Comparison of the model predictions with experimental observations gives for the first time semiquantitative values for the scavenging of the $H_2O^{•+}$ radical in highly concentrated solutions. The estimated contributions of the $H_2O^{•+}$ radical to form the oxidized species $H_2PO_4^•$, $SO_4^{•-}$, $Cl^•$, and $Br^•$ result in α values of 0.26, 0.68, 0.92, and 0.97 for the fraction of $H_2O^{•+}$ radicals that react with the solute. One would like to be able to predict the relative scavenging efficiency of the $H_2O^{•+}$ radical with other solutes. The trend to scavenge the $H_2O^{•+}$ radical depends on the competition between proton transfer by the $H_2O^{•+}$ radical and water (with a rate constant of k_{pt}) and electron transfer by the $H_2O^{•+}$ radical and the solute (with a

DOI: 10.1021/acs.jpca.5b07601
J. Phys. Chem. A 2015, 119, 10629−10636

rate constant of k_{et}). By considering a oversimplified kinetics model the following equation can be used

$$\alpha \approx \frac{k_{et}[H_2O^+][S]}{k_{pt}[H_2O^+][H_2O]} = \frac{k_{et}[S]}{k_{pt}[H_2O]} = \frac{k_{et}}{k_{pt}}R^{-1} \quad (10)$$

The value of α is higher when the concentration of the solute increases. In eq 10 the recombination reactions of electrons with $H_2O^{\bullet+}$ radical in highly concentrated solutions are not considered. This process is also in competition with the scavenging reaction of $H_2O^{\bullet+}$. Moreover, second-order kinetics is used to describe the reaction of $H_2O^{\bullet+}$ radical with neighboring water molecules and solutes; however, these reactions are much more complex and depend on how the positive charge of $H_2O^{\bullet+}$ radical is distributed. Equation 10 can give us an indication of the competition between electron and proton transfer reactions involving $H_2O^{\bullet+}$ radical. Table 1 reports the molar ratio $R = [H_2O]/[S]$ for each studied solution. Solutions of NaCl and NaBr examined here have R values of 8.9 and 7.2, respectively. According to these results, the electron reaction is favored in the case of Br^- solution containing fewer water molecules, resulting in a higher value of α than observed in the Cl^- solution; however, the electron-transfer rate constants between the $H_2O^{\bullet+}$ radical and Cl^- or Br^- may not be the same.

The associated redox potentials of the solutes can be important in predicting the electron-transfer reaction rate constant. The appropriate redox potentials for Br^- and Cl^- solutions are E° ($Br^\bullet/Br^-$) = 1.93 V vs NHE and E° ($Cl^\bullet/Cl^-$) = 2.41 V vs NHE.[30] If one considers that the redox potential for the $H_2O^{\bullet+}$ radical is very high, then again the driving force for the oxidation reaction by the hole is in favor of Br^- system. In fact, the high value of α observed in the Br^- system is in agreement with these predictions. This system also required a very high value for the direct ionization of Br^- to correctly fit the observed data. The results suggest that electron transfer between the $H_2O^{\bullet+}$ radical and Br^- is really efficient and that for the Cl^- is only slightly less.

Concentrated acidic solutions of sulfate and phosphate systems behave differently than those for the halides. According to the values of R and the redox potentials (E° (PO_4^{2-}/PO_4^{3-}) = 2.26 V vs NHE and E° ($SO_4^{\bullet-}/SO_4^{2-}$) = 2.43 V vs NHE),[2] the electron transfer should be more efficient in the case of phosphate, which is not in agreement with the experimental results. In fact, the main reason for the discrepancy is that the phosphate at high concentrations does not exist as a simple PO_4^{3-} but as a dimer ($P_2O_8H_5^-$) and as even more complex species. Therefore, the probability that $H_2O^{\bullet+}$ radical is formed in close proximity to a phosphate group is much lower than that predicted by the value of R. Electron transfer from a phosphate group to the $H_2O^{\bullet+}$ radical is not favored, which explains the low value of α for this system.

The present work clearly shows the contribution of the $H_2O^{\bullet+}$ radical to the ultrafast oxidation processes in concentrated solutions, and the kinetic simulations gives quantitative information on the participation of this radical in the oxidation process. The probability for this oxidation pathway to occur depends on the nature of the solute in aqueous solutions.

AUTHOR INFORMATION

Corresponding Author

*E-mail: mehran.mostafavi@u-psud.fr.

Notes

The authors declare no competing financial interest.

ACKNOWLEDGMENTS

J.A.L. acknowledges the support from the University of Paris-Sud for a visiting position to develop the diffusion-kinetic models. His research described herein was also supported through the Division of Chemical Sciences, Geosciences and Biosciences, Basic Energy Sciences, Office of Science, United States Department of Energy through grant number DE-FC02-04ER15533. This is contribution number NDRL 5080 from the Notre Dame Radiation Laboratory.

REFERENCES

(1) *Recent Trends in Radiation Chemistry*; Wishart, J. F., Rao, B. S. M., Eds.; World Scientific: Singapore, 2010.

(2) Jiang, P.-Y.; Katsumura, Y.; Domae, M.; Ishikawa, K.; Nagaishi, R.; Ishigure, K.; Yoshida, Y. Pulse Radiolysis Study of Concentrated Phosphoric Acid Solutions. *J. Chem. Soc., Faraday Trans.* **1992**, *88*, 3319−3322.

(3) Jiang, P.-Y.; Katsumura, Y.; Nagaishi, R.; Domae, M.; Ishikawa, K.; Ishigure, K.; Yoshida, Y. Pulse Radiolysis Study of Concentrated Sulfuric Acid Solutions. *J. Chem. Soc., Faraday Trans.* **1992**, *88*, 1653−1658.

(4) Balcerzyk, A.; LaVerne, J. A.; Mostafavi, M. Direct and Indirect Radiolytic Effects in Highly Concentrated Aqueous Solutions of Bromide. *J. Phys. Chem. A* **2011**, *115*, 4326−4333.

(5) El Omar, A. K.; Schmidhammer, U.; Rousseau, B.; La Verne, J. A.; Mostafavi, M. Competition Reactions of H2O$^{\bullet+}$ Radical in Concentrated Cl^- Aqueous Solutions: Picosecond Pulse Radiolysis Study. *J. Phys. Chem. A* **2012**, *116*, 11509−11518.

(6) El Omar, A. K.; Schmidhammer, U.; Balcerzyk, A.; La Verne, J. A.; Mostafavi, M. Spur Reactions Observed by Picosecond Pulse Radiolysis in Highly Concentrated Bromide Aqueous Solutions. *J. Phys. Chem. A* **2013**, *117*, 2287−2293.

(7) Garrett, B. C.; Dixon, D. A.; Camaioni, D. M.; Chipman, D. M.; Johnson, M. A.; Jonah, C. D.; Kimmel, G. A.; Miller, J. H.; Rescigno, T. N.; Rossky, P. J.; et al. The Role of Water on Electron-Initiated Processes and Radical Chemistry: Issues and Scientific Advances. *Chem. Rev.* **2005**, *105*, 355−389.

(8) Abramczyk, H. Absorption Spectrum of the Solvated Electron. 1. Theory. *J. Phys. Chem.* **1991**, *95*, 6149−6155.

(9) Webster, F.; Schnitker, J.; Friedrichs, M.; Friesner, R. A.; Rossky, P. J. Solvation Dynamics of the Hydrated Electron. *Phys. Rev. Lett.* **1991**, *66*, 3172−3175.

(10) De Waele, V.; Lampre, I.; Mostafavi, M. Time-Resolved Study on Nonhomogeneous Chemistry Induced by Ionizing Radiation with Low Energy Transfer in Water and Polar Solvents at Room Temperature. In *Charged Particle and Photon Interactions with Matter*; Hatano, Y., Katsumura, Y., Mozumder, A., Eds.; CRC Press: New York, 2010; pp 289−324.

(11) Khorana, S.; Hamill, W. H. Electronic Processes in Pulse Radiolysis of Aqueous Solutions of Halide Ions. *J. Phys. Chem.* **1971**, *75*, 3081−3088.

(12) Kim, K. J.; Hamill, W. H. Direct and Indirect Effects in Pulse Irradiated Concentrated Aqueous-Solutions of Chloride and Sulfate-Ions. *J. Phys. Chem.* **1976**, *80*, 2320−2325.

(13) La Vere, T.; Becker, D.; Sevilla, M. D. Yields of OH in Gamma-irradiated DNA as a Function of DNA Hydration. *Radiat. Res.* **1996**, *145*, 673−680.

(14) Ma, J.; Schmidhammer, U.; Mostafavi, M. Picosecond Pulse Radiolysis of Highly Concentrated Sulfuric Acid Solutions: Evidence for the Oxidation Reactivity of Radical Cation H_2O^+. *J. Phys. Chem. A* **2014**, *118*, 4030−4037.

(15) Ma, J.; Schmidhammer, U.; Mostafavi, M. Picosecond Pulse Radiolysis of Highly Concentrated Phosphoric Acid Solutions:

DOI: 10.1021/acs.jpca.5b07601
J. Phys. Chem. A 2015, 119, 10629−10636

Mechanism of Phosphate Radical formation. *J. Phys. Chem. B* **2015**, *119*, 7180−7185.
(16) Balcerzyk, A.; Schmidhammer, U.; Horne, G.; Wang, F.; Ma, J.; Pimblott, S. M.; de la Lande, A.; Mostafavi, M. Unexpected Ultrafast Silver Ion Reduction: Dynamics Driven by the Solvent Structure. *J. Phys. Chem. B* **2015**, *119*, 10096−10101.
(17) Migus, A.; Gauduel, Y.; Martin, J. L.; Antonetti, A. Excess Electrons in Liquid Water: First Evidence of a Prehydrated State with Femtosecond Lifetime. *Phys. Rev. Lett.* **1987**, *58*, 1559−1562.
(18) Gauduel, Y.; Pommeret, S.; Migus, A.; Yamada, N.; Antonetti, A. Femptosecond Spectroscopy of an Encounter Pair Radical $(H_3O^+...e^-)_{hyd}$ in Concentrated Aqueous Solution. *J. Am. Chem. Soc.* **1990**, *112*, 2925−2931.
(19) Belloni, J.; Monard, H.; Gobert, F.; Larbre, J. P.; Demarque, A.; De Waele, V.; Lampre, I.; Marignier, J. L.; Mostafavi, M.; Bourdon, J. C.; et al. ELYSE - A Picosecond Electron Accelerator for Pulse Radiolysis Research. *Nucl. Instrum. Methods Phys. Res., Sect. A* **2005**, *539*, 527−539.
(20) Schmidhammer, U.; El Omar, A. K.; Balcerzyk, A.; Mostafavi, M. Transient Absorption Induced by a Picosecond Electron Pulse in the Fused Silica Windows of an Optical Cell. *Radiat. Phys. Chem.* **2012**, *81*, 1715−1719.
(21) Muroya, Y.; Lin, M.; Wu, G.; Iijima, H.; Yoshii, K.; Ueda, T.; Kudo, H.; Katsumura, Y. A Re-evaluation of the Initial Yield of the Hydrated Electron in the Picosecond Time Range. *Radiat. Phys. Chem.* **2005**, *72*, 169−172.
(22) Chance, E. M.; Curtis, A. R.; Jones, I. P.; Kirby, C. R. *Report AERE-R 8775*; AERE: Harwell, U.K., 1977.
(23) LaVerne, J. A.; Pimblott, S. M. Scavenger and Time Dependences of Radicals and Molecular Products in the Electron Radiolysis of Water - Examination of Experiments and Models. *J. Phys. Chem.* **1991**, *95*, 3196−3206.
(24) El Omar, A. K.; Schmidhammer, U.; Jeunesse, P.; Larbre, J.-P.; Lin, M.; Muroya, Y.; Katsumura, Y.; Pernot, P.; Mostafavi, M. Time-Dependent Radiolytic Yield of OH Radical Studied by Picosecond Pulse Radiolysis. *J. Phys. Chem. A* **2011**, *115*, 12212−12216.
(25) Ershov, B. G.; Kelm, M.; Janata, E.; Gordeev, A. V.; Bohnert, E. Radiation-Chemical Effects in the Near-Field of a Final Disposal Site: Role of Bromine on the Radiolytic Processes in NaCl-Solutions. *Radiochim. Acta* **2002**, *90*, 617−622.
(26) Bielski, B. H. J.; Cabelli, D. E.; Arudi, R. L.; Ross, A. B. Reactivity of HO_2/O_2^- Radicals in Aqueous Solution. *J. Phys. Chem. Ref. Data* **1985**, *14*, 1041−1100.
(27) Neta, P.; Huie, R. E.; Ross, A. B. Rate Constants for Reactions of Inorganic Radicals in Aqueous-Solution. *J. Phys. Chem. Ref. Data* **1988**, *17*, 1027−1284.
(28) Nielsen, S. O.; Michael, B. D.; Hart, E. J. Ultraviolet Absorption Spectra of e_{aq}^-, H, OH, D, and OD from Pulse Radiolysis of Aqueous Solutions. *J. Phys. Chem.* **1976**, *80*, 2482−2488.
(29) Thomas, J. K.; Rabani, J.; Matheson, M. S.; Hart, E. J.; Gordon, S. Absorption Spectrum of the Hydroxyl Radical. *J. Phys. Chem.* **1966**, *70*, 2409−2410.
(30) Schwarz, H. A.; Dodson, R. W. Equilibrium between Hydroxyl Radicals and Thallium (II) and theOxidation Potential of OH(aq). *J. Phys. Chem.* **1984**, *88*, 3643−3647.

DOI: 10.1021/acs.jpca.5b07601
J. Phys. Chem. A 2015, 119, 10629−10636